FROST FORMATION UNDER DIFFERENT GASEOUS ATMOSPHERES

SATOSHI FUKADA, HISANORI TSURU AND
MASABUMI NISHIKAWA
Department of Nuclear Engineering, Kyushu University, Hakozaki, Higashi-ku, Fukuoka 812-81

Key Words: Mass Transfer, Heat Transfer, Natural Convection, Frost Formation, Frost Thermal Conductivity, Hydrogen

Rates of water frost growth in a vessel with a cooled horizontal plate were experimentally determined under reduced pressure atmospheres of hydrogen, helium, methane and nitrogen. The mass deposited on the cooled surface under each of the atmospheres was almost in proportion to time. The Sherwood number under the condition of no mist formation, Sh_0, in the atmospheres of methane and nitrogen was in good agreement with Catton's equation for natural convection between horizontal parallel plates. Sh_0 in a hydrogen atmosphere was unity, which corresponds to control by molecular diffusion in the stagnant gas. The tendency of the decrease in Sh due to mist formation could be evaluated well by multiplying Sh_0 by a factor ζ_{CSM}. The ζ_{CSM} value was calculated based on the critical supersaturation model as a function of the two interface temperatures and the total pressure. Frost growth rates under each atmosphere were in proportion to $[(T_{S1}-T_{W1})\,t\,/\,(1+1\,/\,A_{S1})]^{0.5}$. The proportional constant for hydrogen was greater than that for any other tested gas. Agreement and disagreement of the frost effective thermal conductivity with previous models were discussed.

Introduction

A cryogenic freezer is supposed to be used for the continuous removal of gaseous impurities, including elements such as carbon, nitrogen, oxygen and helium, from the exhaust stream of a fusion reactor. For a basic study of the cryogenic freezer, we determined rates of frost deposition and growth under reduced nitrogen pressure (Fukada *et al.*, 1995). The experimental apparatus used had a flat cylindrical structure where an upper plate was cooled at a constant temperature and water was evaporated from a lower surface. We elucidated characteristics of frost formation under natural convection and the effect of water mist formation on the mass deposition rate. The experimental Sh values were found to fit to a correlation by Catton *et al.* (1967) for natural convection between horizontal parallel plates multiplied by a factor denoted by ζ_{CSM}. The factor ζ_{CSM} was a parameter defined as a function of the two interface temperatures and the total pressure based on the critical supersaturation model (CSM) (Fukada *et al.*, (1989a,b)). The thickness of frost forming on the cooled plate in the nitrogen atmosphere was in proportion to $[(T_{S1}-T_{W1})\,t]^{0.5}$. The dependence of the frost growth rate on the total pressure was also correlated using another parameter A_{S1}, which was defined as the ratio of latent heat flux to sensitive heat flux on the frost surface.

In the present paper, variations of the mass flux, the total heat flux, the frost thickness and the frost effective thermal conductivity with the temperatures of the upper and lower surfaces are investigated under conditions of reduced pressure of hydrogen, helium, methane or nitrogen using the same experimental apparatus. Results obtained are compared and correlated in a similar way to our previous study (Fukada *et al.*, (1995)). One aim of the present study is to investigate whether the previous results obtained in the nitrogen atmosphere are applicable to frost formation in different atmospheres connected with the fusion fuel clean-up system. Another one is to correlate the frost properties of the effective thermal conductivity and the average density in different gas atmospheres, which has never been investigated before.

1. Experimental

The experimental apparatus and procedures are the same as our previous ones (Fukada *et al.*, (1995)). Therefore, a brief description only is given here. The frosting container has a flat cylindrical structure which is composed of upper and lower stainless-steel plates and a side glass wall. The upper and lower plates are maintained at constant temperature by cooling and heating. The vessel is 400 mm in diameter and 50 mm in height. Each of the cooling and heating temperatures was determined as an arithmetic mean of measurements at several fixed points. The temperatures on the upper and lower plates were uniform and constant in each run. The heat flux through the upper plate was determined using nine thermocouples of 1.5 mm in diameter inserted in the plate. Temperature difference data at three locations of 30 mm, 69 mm and 100 mm from the center assured uniformity of the heat flux over the plate. The temperature profile in liquid water on the lower plate was determined using four thermocouples of

*1) Received April 17, 1995. Correspondence concerning this article should be addressed to S. Fukada.

*2) H.Tsuru is now with Kyushu Electric Power Company, Fukuoka 812.

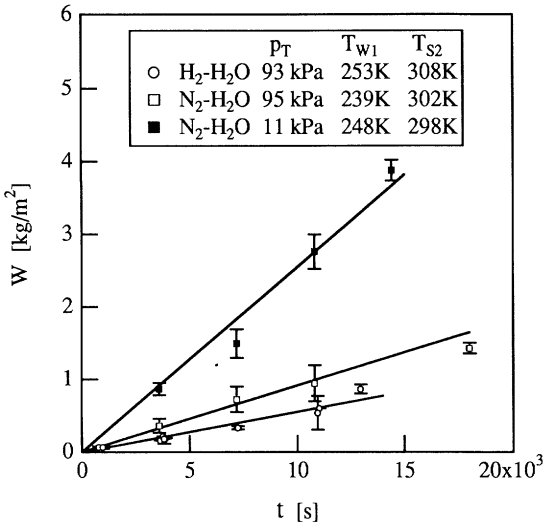

Fig. 1 Variations of mass deposited on cooled surface in atmospheres of hydrogen and nitrogen with time

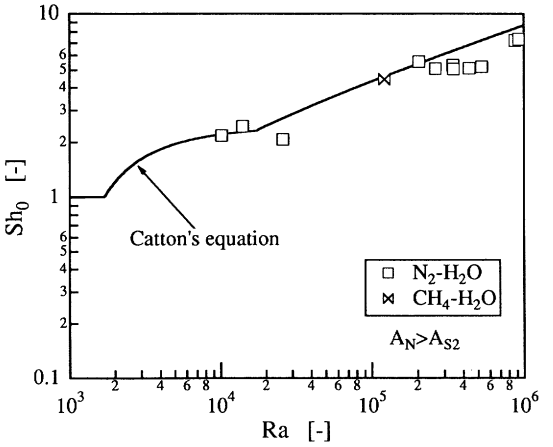

Fig. 2 Comparison between experimental Sh_0 at no mist condition under atmospheres of nitrogen and methane and Catton's equation for natural convection

0.5 mm in diameter fixed at different heights. Temperatures of the frost inside, as well as on the interface, were also determined using five thermocouples of 0.5 mm in diameter fixed at different heights. One may have some problems with interpolation of frost surface temperature by use of fixed thermocouples. However, the temperature profile near the interface was almost linear and no appreciable effect of their interfering in frost and mist formation was observed at this stage of the present study.

Atmospheric gases used are hydrogen, helium, methane and nitrogen. At first, each of the gases was introduced up to a specified pressure into the vessel which was evacuated beforehand by using vacuum pumps. Then, distilled water having somewhat higher temperature than that of the lower heated plate was introduced into the container. The amount of mass deposited and the frost thickness after an elapse of frosting time were determined at several points on the upper cooled plate. The arithmetic mean of their data was correlated for the present analysis.

The ranges of the upper and lower plate temperatures and the total pressure in this experiment were 200 K < T_{W1} < 266 K, 290 K < T_{S2} < 323 K and 8 kPa < p_T < 100 kPa.

2. Results and Discussion

2.1 Rate of mass deposition, j_M

Figure 1 shows variations of the mass deposited per unit surface area, W, under atmospheres of hydrogen and nitrogen with frosting time, t. Experimental errors were evaluated from differences in the deposited amount at various points of measurement. Although the errors were different from experiment to experiment, their maximum was 10 %. The obtained W values were almost in proportion to time in a similar way to previous investigations (Brian *et al.*, (1970) and Fukada *et al.*, (1995)). It was expected that the mass deposition rate, j_M, varies with the frosting time due to a decrease in the driving force of the concentration between the lower and upper interfaces. The degree of the decrease was evaluated as 10 % at most under the experimental conditions in the figure. Since j_M is also affected by roughness of frost surfaces, the decrease might be hidden within error bars. Generally speaking, frosting is a complicated phenomenon which proceeds in relation with both amounts accumulated till a specified time, *e.g.*, l_F and ρ_F and rates at the time, *e.g.*, j_M and q_H. For the sake of convenience, in calculating A_{S1} explained later, j_M was treated as a constant.

Judged from the interface temperatures, the density of the mixture of hydrogen and water vapor on the lower interface is higher than that on the upper one. This is because the molecular weight of hydrogen is much lighter than that of water. Therefore, no natural convection occurred in the vessel. This was assured also from the fact that there was no oscillation of bulk temperatures in the hydrogen atmosphere. Consequently, only molecular diffusion in the stagnant hydrogen transferred water vapor from the lower surface to the upper one.

On the other hand, oscillations of the gaseous temperature were generated under the atmospheres of nitrogen, methane and, in some cases, helium. The presence of temperature oscillations suggested that natural convection, *i. e.*, Rayleigh-Benard convection, controls the transfer of water vapor between the horizontal plates. As seen in Fig. 1, natural convection enhanced the mass deposition rate under the nitrogen atmosphere compared with the case of hydrogen. In order to rate the degree of natural convection, Ra for simultaneous heat and mass transfer was calculated based on the definition (Eckert, (1981) and Fukada *et al.*, (1995)).

Figure 2 shows variations of Sh_0 with Ra in the atmospheres of nitrogen and methane under no mist formation. The Sherwood number was calculated using j_M at the initial stage of the frost formation and that under no mist formation is indicated as Sh_0 in the present study. The logarithmic difference between the vapor pressures on the upper and lower interfaces was adopted for the driving force of mass transfer. As seen in the figure, the experimental Sh_0 values fitted the correlation for natural

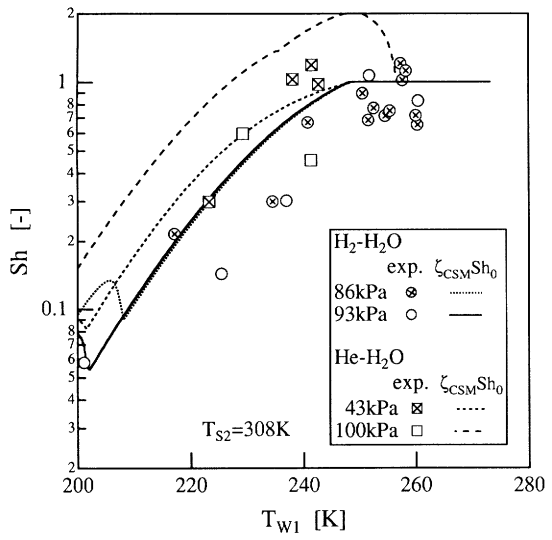

Fig. 3 Comparison between experimental *Sh* under the condition of mist formation under atmospheres of hydrogen and helium and calculation values based on CSM

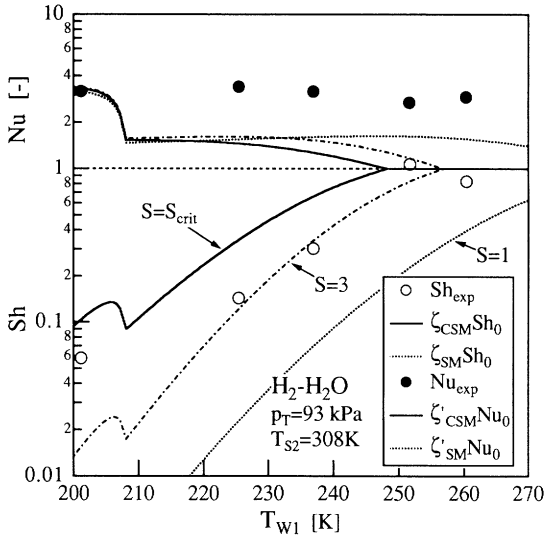

Fig. 4 Variations of *Sh* and *Nu* with cooled surface temperature and the calculation values

convection by Catton *et al.* (1967). There is some possibility that the critical *Ra* for the simultaneous heat and mass transfer is different from the value of 1707 given for pure natural convection. However, the relation between *Ra* and Sh_0 obtained here clearly revealed characteristics of the mass-transfer process in the enclosed vessel.

A_N and A_{S2} are parameters calculated from the interface temperatures and properties of the gas mixture to predict whether mist is generated in a system or not. T_N or y_N ($= y_{crit}(T_N)$) appearing in the definition of A_N is a parameter defined as temperature or mass fraction of vapor on a nucleation boundary. Both are calculated from the tangency condition:

$$\left(\frac{dy_{crit}}{dT}\right)_{T=T_N} = \frac{y_N - y_{S2}}{T_N - T_{S2}} \tag{1}$$

The critical condition for mist formation is expressed by the relation $A_N = A_{S2}$, and the condition of $A_N < A_{S2}$ predicts that mist is generated in the system (Fukada *et al.*, (1989a,b)).

Figure 3 shows variations of *Sh* with the temperature of the cooled plate, T_{W1}, in atmospheres of hydrogen and helium. With lowering T_{W1}, *Sh* begins to decrease due to water mist generation and, consequently, a drop in water vapor pressure. The cooling temperature where *Sh* starts decreasing almost corresponded to one predicted from CSM.

Each curve in the figure was calculated by multiplying Sh_0 by a factor ζ_{CSM} calculated from CSM for respective gas-water systems. As mentioned above, no natural convection occurred for hydrogen. Therefore, Sh_0 was theoretically unity. On the other hand, comparatively small convection was generated for helium below 260 K at 100 kPa, and so the maximum value appears in the calculation curve of *Sh* at around 250 K. As seen in the figure, CSM could qualitatively predict the degree of the decrease in *Sh* due to mist formation under each atmosphere. However, the experimental values were not quantitatively consistent with the CSM calculations. There were larger deviations in the H_2-H_2O system. In order to clarify the cause of the deviations, an evaluation was made based on supplementary calculations as follows.

Figure 4 shows variations of *Nu* and *Sh* at the initial frosting period with T_{W1} under a hydrogen atmosphere at 93 kPa. Although the experimental *Sh* values were not well estimated by the saturation model depicted by $S = 1$ as well as by CSM, they were in comparatively good agreement with ones calculated by using $S = 3$. Thus, the deviations from CSM could be compensated to some extent by taking into consideration the fact that mist generating at the critical supersaturation condition grows up with its falling down in the vessel. This is because mist grows in diameter with diffusion of water vapor and it decreases the degree of the supersaturation. However, the value of $S = 3$ obtained here is considered to be only an empirical constant.

2.2 Nusselt number, *Nu*

The experimental *Nu* values shown in Fig. 4 were around two times larger than the values of Nu_0 multiplied by a factor calculated by CSM or $S = 3$, which are denoted by $\zeta'_{CSM}Nu_0$ or $S = 3$. The Nu_0 value corresponding to thermal conduction in the stagnant gas is equal to unity in a similar way to Sh_0.

In order to trace to the origin of the differences in *Nu* between the experimental and calculational values, contributions of radiation heat transfer between the parallel plates were estimated. Here, we take an example of a H_2-H_2O system at $T_{S2} = 308$ K, $T_{S1} = 243$ K and $p_T = 93$ kPa. The contribution of radiation from the gas mixture evaluated using the correlations by Schack (Japan Society of Mechanical Engineers, (1975)) and Ushikin and Sparrow (1960) was found to be negligible in this system. Next, the radiative heat-transfer rates among the two plates and the side wall were calculated using Kirchhoff's law. The radiative transfer rate through the upper plate so obtained was

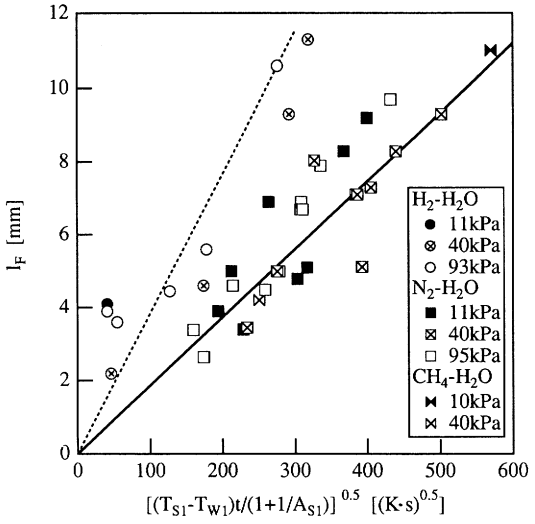

Fig. 5 Variations of frost thickness under atmospheres of hydrogen, nitrogen and methane with $[(T_{S1}-T_{W1})t/(1+1/A_{S1})]^{0.5}$

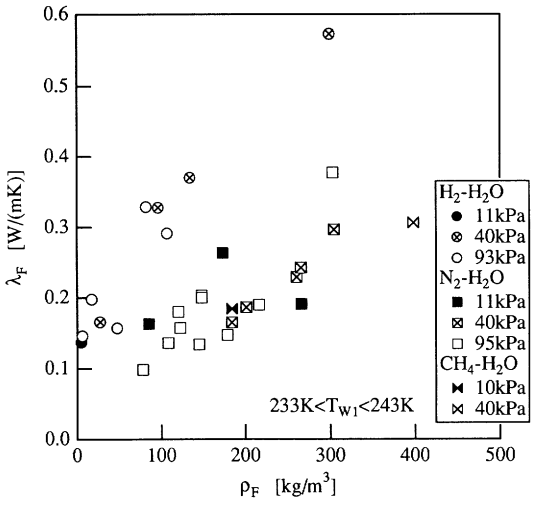

Fig. 6 Variations of effective thermal conductivity of frost with average frost density under atmospheres of hydrogen, nitrogen and methane

223 W/m^2 by use of $\varepsilon_1 = 0.98$ (Yamakawa *et al.*, (1969)), $\varepsilon_2 = 0.96$, $\varepsilon_3 = 0.94$ and $F_{12} = 0.12$ (Japan Society of Mechanical Engineering, (1975)). The rate was comparative with an addition of the convective heat-transfer rate and the latent heat-transfer rate. This resulted in the experimental *Nu* being around two times larger than the calculated *Nu*. Thus, the radiative heat transfer rate made up for the differences in *Nu* to a certain extent. However, no correction for the radiative heat transfer was done here because the rate is very sensitive to the frost emissivity and there was the possibility that the emissivity varies with different frost structures in different atmospheres.

A combination of the present results and our previous papers (Fukada *et al.*, (1989a,b, 1995)) leads to the conclusion that CSM can successfully describe the mass-transfer process not only under forced convection but also under natural convection with some modifications. Hence, CSM serves a useful way to estimate any mass-transfer rate under mist formation.

Variations of q_H with frosting time were not quantitatively elucidated in the present paper. This is because q_H was affected more heavily by phenomena such as rise in the surface temperature and change of the frost surface roughness than j_M.

2.3 Frost thickness, l_F

Figure 5 shows a comparison of the frost thickness, l_F, under the reduced atmospheres of hydrogen, nitrogen and methane. In order to avoid confusion, the same marks are used for the data of respective gases regardless of mist formation. The dotted line was drawn from fitting to hydrogen data. The solid line was drawn with the same slope as the previous results for nitrogen (Fukada *et al.*, (1995)). The latter was also consistent with the present nitrogen data. Thus, the growth rate in each atmosphere was in proportion to $[(T_{S1}-T_{W1})\,t\,/\,(1+1\,/\,A_{S1})]^{0.5}$ regardless of p_T. This reveals that A_{S1} in the lump variable is a feasible parameter to correlate l_F under various pressures.

The proportional constant was related to a presumed linearity of the effective thermal conductivity of frost, λ_F, versus the average frost density, ρ_F, (Fukada *et al.*, (1995)). The proportional constant for hydrogen was the largest, and the value was 0.037 mm/(Ks)$^{0.5}$. That for nitrogen was 0.019 mm/(Ks)$^{0.5}$. Although there are only two data for methane, they are in the range of scattering of the data for nitrogen. The gaseous thermal conductivity, λ_g, is 0.17 W/(mK) for hydrogen, 0.024 W/(mK) for nitrogen and 0.030 W/(mK) for methane at 100 kPa. Thus, the proportional constant is associated with λ_g. Since the proportional constant, however, should be directly correlated by λ_F, it was experimentally investigated as follows.

2.4 Effective thermal conductivity of frost, λ_F

λ_F is one of the most important frost properties and is defined by the equation (Biguria and Wenzel (1970)):

$$\lambda_F = \frac{q_T l_F}{T_{S1} - T_{W1}} \tag{2}$$

Figure 6 shows a comparison among λ_F values under the reduced pressures of hydrogen, nitrogen and methane. Although λ_F values under an atmospheric pressure were presented by various investigators (Biguria and Wenzel (1970), Dietenberger (1983), Hayashi *et al.* (1977) and Woodside (1958)), no work has been done on λ_F under reduced pressure of atmospheric gases other than air. The λ_F values in the hydrogen atmosphere are greater than those in the nitrogen or methane atmosphere. This is because λ_g of hydrogen gas is largest. The order of the λ_F values in different atmospheres at a specified ρ_F was consistent with that of the proportional constant of l_F. Another thing to be noticed in the figure is that λ_F under each of the atmospheres is almost independent of p_T.

There were many models to evaluate λ_F from λ_g, ρ_F, porosity and so on. In order to evaluate λ_F of growing frost, Biguria and Wenzel (1970), Hayashi *et al.* (1977) and Woodside (1958) introduced the concept of the effective thermal conductivity of gas, $\lambda_{g,\,diff}$, in place of λ_g in their models:

$$\lambda_{g,\,diff} = \lambda_g + \lambda_{diff} \tag{3}$$

λ_{diff} was then evaluated by the equation:

$$\lambda_{diff} = \frac{D_{AB} p_T L_V}{R_g T (p_T - p_{sat})} \left(\frac{dp_{sat}(T)}{dT} \right) \quad (4)$$

Thus, $\lambda_{g,\,diff}$ was defined as a simple addition of the thermal conductivity of the atmospheric gas and the contribution of the diffusion rate of water vapor through frost.

We compared our experimental λ_F values with the series resistance model, the parallel resistance model, the model by Maxwell and Rayleigh (Biguria and Wenzel (1970)), that by Brailsford and Major (1964), and that by Woodside (1958). If Eq. (4) was used for λ_{diff}, the calculation results, unfortunately, failed to predict the experimental results of Fig. 6. This was because the calculated λ_F depended heavily on p_T due to the fact that the molecular diffusion coefficient, D_{AB}, in Eq.(4) is inversely proportional to p_T. Therefore, if Eq.(3) holds, other mechanisms of water diffusion and frost internal growth are necessary for the explanation of experimental λ_F independent of p_T.

In addition to that, there was another unsolved problem from previous experimental results (Brian *et al.*, (1970)) - to show that the local frost density was uniform in the direction of frost growth. The frost uniformity was qualitatively observed through a borescope in the present experiment. If water vapor diffuses in the inside of frost at the condition of critical supersaturation or saturation, an exponential-like variation of the vapor pressure along the direction of the frost height is expected from a linear temperature profile. The variation of the local frost density with time is in proportion to the space differential of the vapor pressure profile. Therefore, the exponential-like profile is inconsistent with the uniformity of the local frost density.

The macroscopic frost growth rate has been successfully described by use of the overall heat and mass balance equations. However, the microscopic frost growth was inconsistent with the usual balance equations. Water vapor over the critical supersaturation condition is present as water mist in porous frost. Consequently, thermophoretic and diffusionphoretic forces might work on water mist and might affect the mass-transfer rate of water. In addition to this, frost had a dendrite structure in this experimental condition. Therefore, the microscopic frost growth may be affected by the fractal performance of crystal growth as well. At this stage of the present study, unfortunately, we could not quantitatively describe the microscopic frost growth process. Therefore, the problem of the λ_F independence of p_T was not solved. In order to make it clear, further work will have to be done.

Conclusions

The mass deposited under reduced pressure of hydrogen, helium, methane or nitrogen was satisfactory correlated with the Sherwood number. The Sh_0 values when

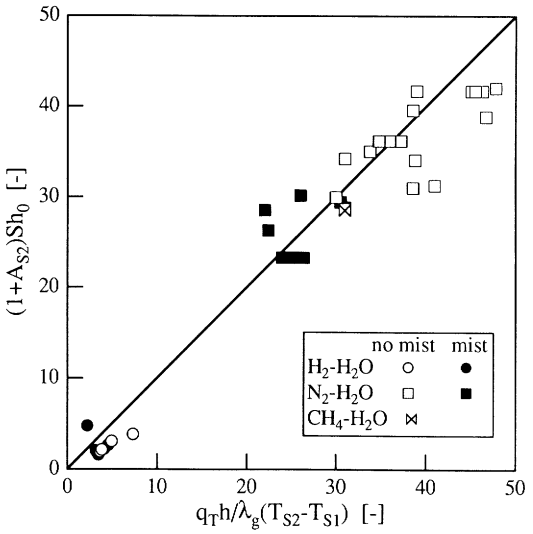

Fig. A1 Relation between $q_T h/\lambda_g (T_{S2}\text{-}T_{S1})$ and $(1+A_{S2})\, Sh_0$

$A_N > A_{S2}$, *i.e.*, under the condition of no mist formation, were in good agreement with Catton's correlation for natural convection. The Sh values when $A_N < A_{S2}$, *i.e.*, under the condition of mist formation, were well evaluated by multiplying the Sh_0 value by a factor ζ_{CSM} based on CSM with some modifications. This implies that the degree of supersaturation is independent of atmospheric gases and convection modes. Frost growth rates under any of the atmospheres were in proportion to $[(T_{S1}\text{-}T_{W1})\, t / (1 + 1 / A_{S1})]^{0.5}$ regardless of mist formation. The order of the proportional constants was consistent with the order of λ_F. Thus, characteristics of the frost growth rate and the heat flux at reduced pressure in different atmospheres were understood in an extended frame of our previous knowledge on the heat and mass transfer phenomena between horizontal plates.

λ_F obtained under reduced pressures varied with ρ_F and the kind of gases. The λ_F dependence on ρ_F was understood in a similar way to previous models. However, the λ_F independence of p_T could not be explained by use of $\lambda_{g,\,diff}$. Another explanation for the λ_F independence of p_T and the space uniformity of the local frost density is required.

Appendix; Dimensionless total heat flux

The total heat flux under the condition of no mist formation, $q_{T,0}$, is expressed by the equation:

$$q_{T,0} = q_{H,0} + L_V j_{M,0} \quad (A1)$$

Sh_0 and Nu_0 under the condition of no mist formation are defined by the equation:

$$Sh_0 = \frac{j_{M,0}\, h}{\rho_g D_{AB} \ln\left(\frac{1 - y_{S1}}{1 - y_{S2}}\right)} \quad (A2)$$

$$Nu_0 = \frac{q_{M,0}\, h}{\lambda_g (T_{S2} - T_{S1})} \quad (A3)$$

Substituting Eqs. (A2) and (A3) into Eq. (A1) leads to the equation.

$$Nu_{T,0} = Nu_0 + A_{S2}Sh_0 \quad \text{(A4)}$$

If one assumes $Nu_0 = Sh_0$, $Nu_{T,0} = (1 + A_{S2})\ Sh_0$ holds.

The dimensionless total heat flux, $q_T h / \lambda_g (T_{S2}-T_{S1})$, was theoretically given by $(1 + A_{S2})\ Sh_0$ also under the condition of mist formation (Fukada *et al.*, (1989a,b)). The above two relations enable experimental measurement whether the total heat flux through the upper plate, q_T, is independent of mist formation or not. For calculating A_{S2}, the time constancy of the heat and mass fluxes was here assumed as the first approximation.

Figure A1 shows the relation between $q_T h / \lambda_g (T_{S2}-T_{S1})$ and $(1 + A_{S2})\ Sh_0$ under both mist formation and no mist formation. The results reveal that $(1 + A_{S2})\ Sh_0$ agrees with Nu_T regardless of mist formation. Thus, the basic assumption of CSM that the total heat flux does not change regardless of mist formation (Fukada *et al.*, (1989a, 1984) was experimentally proven.

Nomenclature

A_N	=	$L_V \rho_g D_{AB} \ln \{(1-y_{S1})/(1-y_N)\} / \lambda_g (T_N-T_{S1})$	[-]
A_{S1}	=	Ratio of latent heat flux to sensitive heat flux on frost surface defined by $L_V j_M / q_H$	[-]
A_{S2}	=	$L_V \rho_g D_{AB} \ln \{(1-y_{S1})/(1-y_{S2})\} / \lambda_g (T_{S2}-T_{S1})$	[-]
D_{AB}	=	Diffusion coefficient of water vapor	[m^2s^{-1}]
F	=	Direct view factor	[-]
g	=	Acceleration of gravity	[ms^{-2}]
h	=	Distance between upper frost surface and lower water surface	[m]
j_M	=	Mass flux of water on frost surface	[$kgm^{-2}s^{-1}$]
L_V	=	Latent heat of sublimation	[Jkg^{-1}]
l_F	=	Frost thickness	[m]
M_{S2}	=	Molecular weight of gas mixture on water surface	[$kgmol^{-1}$]
M_{S1}	=	Molecular weight of gas mixture on frost surface	[$kgmol^{-1}$]
Nu	=	Nusselt number defined by $q_H h / \lambda_g (T_{S2}-T_{S1})$	[-]
Nu_T	=	Nusselt number defined by $q_T h / \lambda_g (T_{S2}-T_{S1})$	[-]
p_{sat}	=	Saturation pressure of vapor	[Pa]
p_T	=	Total pressure	[Pa]
q_H	=	Sensitive heat flux on frost surface	[Wm^{-2}]
q_T	=	Total heat flux	[Wm^{-2}]
R_g	=	Gas constant	[$Jkg^{-1}K^{-1}$]
Ra	=	Rayleigh number defined by $gh^3 (T_{S2}M_{S1} / T_{S1}M_{S2}-1) / \upsilon (\kappa D_{AB})^{0.5}$	[-]
S	=	Supersaturation ratio	[-]
Sh	=	Sherwood number defined by $j_M h / \rho_g D_{AB} \ln \{(1-y_{S1}) / (1-y_{S2})\}$	[-]
T	=	Temperature	[K]
T_N	=	Parameter defined as temperature at nucleation boundary	[K]
T_{S1}	=	Temperature of upper frost surface	[K]
T_{S2}	=	Temperature of lower water surface	[K]
T_{W1}	=	Temperature of upper cooled plate	[K]
t	=	Time	[s]
W	=	Mass per unit area deposited on cooled plate	[kgm^{-2}]
y_N	=	Mass fraction of water vapor at nucleation boundary	[-]
y_{S1}	=	Mass fraction of water vapor at frost surface	[-]
y_{S2}	=	Mass fraction of water vapor at water surface	[-]
y_{W1}	=	Mass fraction of water vapor at cooled plate surface	[-]
κ	=	Thermal diffusivity of gas mixture	[m^2s^{-1}]
ζ_{CSM}	=	Factor for mass transfer under mist formation based on CSM defined by $A_N (1+A_{S2}) / A_{S2} (1+A_N)$	[-]
ζ'_{CSM}	=	Factor for heat transfer under mist formation based on CSM defined by $(1+A_{S2}) / (1+A_N)$	[-]
λ_{diff}	=	Thermal conductivity based on water vapor diffusion defined by Eq.(4)	[$Wm^{-1}K^{-1}$]
λ_F	=	Effective thermal conductivity of frost	[$Wm^{-1}K^{-1}$]
λ_g	=	Thermal conductivity of gas mixture	[$Wm^{-1}K^{-1}$]
$\lambda_{g,diff}$	=	Effective thermal conductivity of gas mixture defined by Eq. (3)	[$Wm^{-1}K^{-1}$]
ρ_F	=	Average frost density	[kgm^{-3}]
ρ_g	=	Density of gas mixture	[kgm^{-3}]
υ	=	Kinematic viscosity of gas mixture	[m^2s^{-1}]

<Subscripts>

0	No mist condition
1	Upper interface
2	Lower interface
3	Side wall
cal	Calculation
crit	Critical supersaturation
exp	Experiment
S	Interface
sat	Saturation
W	Wall

Literature Cited

G.B.Biguria and L.A.Wenzel; "Measurement and Correlation of Water Frost Thermal Conduction and Density," *I&EC Fundam.*, **9** (1970) 129-138

A.D.Brailsford and K.J.Major; "The Thermal Conductivity of Aggregates of Several Phases, Including Porous Materials," *Brit. J. Appl. Phys.*, **15** (1964) 313-319

P.L.T.Brian, R.C.Reid and I.Branzinsky; "Frost Deposition on Cold Surfaces," *I&EC Fundam.*, **9** (1970) 375-380

I.Catton and D.K.Edwards; "Effect of Side Walls on Natural Convection between Horizontal Plates Heated from Below," *Trans. ASME*, **C-89** (1967) 295-299

M.A.Dietenberger; "Generalized Correlation of the Water Frost Thermal Conductivity," *Int. J. Heat Mass Transfer*, **26** (1983) 607-619

E.R.G.Eckert; "Pioneering Contributions to Our Knowledge of Conduction Heat Transfer," *Trans. ASME*, **C-103** (1981) 409-414.

S.Fukada, K.Inoue and M.Nishikawa; "Frost Deposition on Cooled Surfaces under Reduced Pressure," *Kagaku-Kougaku Ronbunshu*, **21** (1995) 166-172

S.Fukada, S.Furuta and N.Mitsuishi, "Mass Transfer with Mist Formation for Laminar Flow in Vertical Cooling Tube with Constant Temperature Wall - Experimental and Theoretical Study on Fuel Gas Refining System with Cryogenic Freezer," *J. Atom. Ener. Soc. Japan*, **31** (1989a) 487-496

S.Fukada, K.Inoue and N.Mitsuishi; "Effects of Presence of Foreign Nuclei on Mass Flux at Cooling Walls in Cryogenic Freezer," *J. Nucl. Sci. Technol.*, **26** (1989b) 808-810

S.Fukada and N.Mitsuishi; "Heat and Mass Transfer in a Laminar Boundary Layer under Mist Formation," *Technology Reports on the Kyushu University*, **57** (1984) 9-14

Y.Hayashi, A.Aoki, S.Adachi and K.Hori; "Study of Frost Properties Correlating with Frost Formation Types," *Trans. ASME*, **C-99** (1977) 239-245

The Japan society of the mechanical engineers, "Dennetsu Kougaku Siryou," (1975) 134

C.M.Usiskin, and E.M.Sparrow,"Thermal Radiation between Parallel Plates Separated by an Absorption-Emitting Nonisothermal Gas," *Int. J. Heat Mass Transf.*, **1** (1960) 28-36

W.Woodside; "Calculation of the Thermal Conduction of Porous Media," *Can. J. Phys.*, **36** (1958) 815-823

N.Yamakawa, N.Takahashi and S.Otani, "On the Measurement of the Surface Temperature under the Freezing Condition," *Kagaku Kogaku*, **33** (1969) 699-701